Atmospheric Chemistry and Physics Discussions

Three years of routine Raman lidar measurements of tropospheric aerosols: Planetary boundary layer heights, extinction and backscatter coefficients

J. Schneider[1,*] and R. Eixmann[1]

[1]Leibniz-Institute for Atmospheric Physics at Rostock University, Kühlungsborn, Germany
[*]Present address: Cloud Physics and Chemistry Department, Max-Planck-Institute for Chemistry, Mainz, Germany

Correspondence to: J. Schneider (schneider@mpch-mainz.mpg.de)

Title Page	
Abstract	Introduction
Conclusions	References
Tables	Figures
◄◄	►►
◄	►
Back	Close
Full Screen / Esc	

Print Version

Interactive Discussion

Abstract

We have performed a three-year series of routine lidar measurements on a climatological base. To obtain an unbiased data set, the measurements were taken at preselected times. The measurements were performed between 1 December 1997, and 30 November 2000, at Kühlungsborn, Germany (54°07′ N, 11°46′ E). Using a Rayleigh/Mie/Raman lidar system, we measured the aerosol backscatter coefficients at three wavelengths in and above the planetary boundary layer. The aerosol extinction coefficient has been determined at 532 nm, but here the majority of the measurements has been restricted to heights above the boundary layer. Only after-sunset measurements are included in this data set since the Raman measurements were restricted to darkness. For the climatological analysis, we selected the cloud-free days out of a fixed measurement schedule. The annual cycle of the boundary layer height has been found to have a phase shift of about 25 days with respect to the summer/winter solstices. The mean values of the extinction and backscatter coefficients do not show significant annual differences. The backscatter coefficients in the planetary boundary layer were found to be about 10 times higher than above. The mean aerosol optical depth above the boundary layer and below 5 km is $0.26(\pm 1.0) \times 10^{-2}$ in summer, and $1.5(\pm 0.95) \times 10^{-2}$ in winter, which almost negligible compared to values measured in the boundary layer. A cluster analysis of the backward trajectories yielded two major directions of air mass origin above the planetary boundary layer and 4 major directions inside. A marked difference between the total aerosol load dependent on the air mass origin could be found for air masses originating from the west and travelling at high wind speeds. Comparing the measured spectral dependence of the backscatter coefficients with data from the Global Aerosol Data Set, we found a general agreement, but only a few conclusions with respect to the aerosol type could be draws due to the high variability of the measured backscatter coefficients.

1. Introduction

For the assessment of the climatic impact of aerosols (aerosol forcing) the knowledge of both the temporal and vertical distribution of the aerosol is essential. Lidar can provide vertically resolved measurements of extinction and backscatter coefficients on a long-time basis. However, the retrieval of these optical properties by conventional backscatter lidar suffers from the well known problem that two quantities are calculated from only one measured signal. Therefore, the so-called lidar ratio, i. e. the ratio between aerosol extinction and backscatter coefficient, is needed as an input parameter (e.g. Klett, 1981, 1985; Fernald, 1984). This lidar ratio is usually height- and aerosol type-dependent and can only roughly be estimated for individual measurements. The error introduced by assuming a height-independent lidar ratio was thoroughly discussed by Sasano et al. (1985). A different lidar approach is the use of an second, independent molecular backscatter signal, ususally the Raman-shifted nitrogen backscatter signal. This technique allows the independent determination of the aerosol extinction coefficient (Ansmann et al., 1990, 1992). Furthermore, the backscatter coefficient is determined from the ratio of two return signal which leads to independence of the requirement of a full overlap between laser beam and telescope field-of-view. Due to the low intensity of the Raman scattering, this technique is usually restricted to night-time, when the background from the sky is low enough. Since 1 December 1997, the department "Optical Soundings" at the Leibniz Institute for Atmospheric Physics (IAP) at Kühlungsborn, Germany, performs routine lidar measurements within the German Lidar Network (Bösenberg et al., 1998) and its follow-up project, EARLINET (European Aerosol Lidar Research Network) (Bösenberg et al., 2000). Major goal of both projects is the establishment of an unbiased climatological data set characterizing the vertical distribution of optical aerosol parameters at selected sites. This goal requires random sampling which is not correlated with particular weather situations. To achieve this the routine measurements are performed at preselected times independent from atmospheric conditions. The measured profiles are

J. Schneider and R. Eixmann

Title Page

Abstract   Introduction

Conclusions   References

Tables   Figures

◄   ►│

◄   ►

Back   Close

Full Screen / Esc

Print Version

Interactive Discussion

averaged over at least thirty minutes to reduce the influence of small scale variability. Here, we report the results of the first three years of routine operation at Kühlungsborn (54° N, 12° E), focusing on the Raman measurements after sunset.

2. Measurements

5 2.1. System description

The Rayleigh/Mie/Raman (RMR) lidar at IAP Kühlungsborn uses a Nd:YAG laser system (Spectra Physics GCR 290) emitting at the fundamental (1064 nm) and the second and third harmonic (532 and 355 nm). Detected signals include the three emitted wavelength plus the nitrogen Raman shifted return signals at 607 and 387 nm. Additionally,
10 the vertical depolarized return signal at 532 nm is detected. All signals are detected with 50 m vertical resolution. The receiver site consists of two telescopes (50 cm diameter each) of which the first is mounted coaxially to laser beam and is used for detection of the 355 nm, 532 nm, 1064 nm, and the 607 nm Raman signal. Full geometric overlap is reached at 1000 m, approximately. The second is mounted off-axis and is used
15 for the 387 nm and the depolarized signal. Here, full geometric overlap is reached only at 2000 m, which is in general above the planetary boundary layer. For this reason, no 387 nm data were included in the present work. In the meantime, the 387 nm channel has also been included into the coaxial telescope. The system is located at Kühlungsborn, Germany (54°07′ N, 11°46′ E), in a rural environment near the shore of
20 the Baltic Sea, and is in operation since June 1997 (Alpers et al., 1999). A schematic of the setup, showing only the components used for this work, is given in Fig. 1. In the detection branch the wavelengths are seperated by dichroic beam splitters, filtered using interference filters (Barr Associates, Inc.), and detected by photomultiplier tubes. Technical data of the system are summarized in Table 1.

2.2. Determination of the aerosol optical parameters

Calculation of the extinction coefficient from the Raman signals follows the method described by Ansmann et al. (1990, 1992). The aerosol extinction coefficient $\alpha^{aer}_{\lambda_R}$ at the Raman shifted wavelength λ_R is given by:

$$\alpha^{aer}_{\lambda_R}(z) = \frac{-\frac{d}{dz}\ln\left(P^{korr}_{\lambda_R}(z)\right)}{1 + \left(\frac{\lambda_0}{\lambda_R}\right)^k} \tag{1}$$

where $P^{korr}_{\lambda_R}(z)$ is the detected signal corrected for range, N_2 number density, and molecular extinction:

$$P^{korr}_{\lambda_R}(z) = \frac{P_{\lambda_R}(z)z^2}{N_R(z)\exp\left(-\int_0^z\left[\alpha^{mol}_{\lambda_0}(\zeta) + \alpha^{mol}_{\lambda_R}(\zeta)\right]d\zeta\right)} \tag{2}$$

with:

λ_0:   emitted wavelength
z: altitude,
$P_{\lambda_R}(z)$:   received Raman backscatter signal from the altitude z,
$N_R(z)$:   number density of Raman scatterers, here N_2 molecules
$\alpha^{mol}_{\lambda_0}, \alpha^{mol}_{\lambda_R}$:   molecular extinction at λ_0 and λ_R, respectively.

This method allows one to determine the extinction coefficient independently, with the only necessary assumption of the wavelength dependence of the aerosol extinction coefficient

$$\alpha_{aer}(\lambda) \sim \lambda^{-k}. \tag{3}$$

Since the ratio between emitted and Raman shifted wavelengths is close to unity, deviations of this assumption do not contribute to significant errors. Observations indicate

Raman lidar measurements of tropospheric aerosols

J. Schneider and R. Eixmann

Title Page

Abstract | Introduction

Conclusions | References

Tables | Figures

◄◄ | ►►

◄ | ►

Back | Close

Full Screen / Esc

Print Version

Interactive Discussion

that k varies between 0 and 2 (Ferrare et al., 1998). For cirrus clouds, k equals zero (Ansmann et al., 1992). Usually, $k = 1$ is assumed for all measurements except for cirrus clouds, where $k = 0$ is chosen. To obtain the nitrogen molecule number density and the Rayleigh scattering coefficients $\alpha_{\lambda_0}^{mol}$ and $\alpha_{\lambda_R}^{mol}$, air temperature, density, and relative humidity are available from local radiosonde measurements, performed by the German Weather Service (DWD) on a regular basis. Radiosonde data are available at noon and midnight from two stations, one located 120 km east (Greifswald), the other located 150 north–west (Schleswig). Additionally, on certain occasions radiosondes can be launched at IAP Kühlungsborn. For days where no radiosonde data were available, the US Standard Atmosphere was used. In order to calculate the derivative

$$\frac{d}{dz}\left[\ln\left(PR^2\right)\right],$$

the received Raman signal has to be averaged in time and altitude. To reduce the influence of small scale variability, a minimum time interval of 30 min (approximately 54 000 laser shots) was chosen by the participants of the lidar networks. Typical height intervals are: 200 m (4 channels) between 1 and 5 km, 500 m between 5 and 10 km, and 1000 m above 10 km. These values are subject to change dependent on the actual shape of the lidar return signal, the averaged time interval and thereby the total count rate. Since the method is based on the absolute lidar return signal, it can only be applied above the height at which the laser beam and the telescope field-of-view fully overlap. This reduces our data to altitudes above 1 km, thereby excluding most of the boundary layer. Once the aerosol extinction coefficient is known, the aerosol backscatter coefficient can be determined from the following equation:

$$\beta_{\lambda_0}^{aer}(z) = -\beta_{\lambda_0}^{mol}(z) + \left[\beta_{\lambda_0}^{aer}(z_0) + \beta_{\lambda_0}^{mol}(z_0)\right] \times \frac{P_{\lambda_R}^{korr}(z_0)P_{\lambda_0}^{korr}(z)}{P_{\lambda_0}^{korr}(z_0)P_{\lambda_R}^{korr}(z)} \times \frac{\exp\left[-\int_{z_0}^{z}\alpha_{\lambda_R}^{aer}(\zeta)d\zeta\right]}{\exp\left[-\int_{z_0}^{z}\alpha_{\lambda_0}^{aer}(\zeta)d\zeta\right]} \tag{4}$$

with

$$P_{\lambda_0}^{korr}(z) = \frac{P_{\lambda_0}(z)z^2}{\exp\left(-2\int_0^z \left[\alpha_{\lambda_0}^{mol}(\zeta)\right]d\zeta\right)} \tag{5}$$

and

$P_{\lambda_0}(z)$:   received backscatter signal at λ_0 from the altitude z,

$\beta_{\lambda_0}^{mol}(z)$:   molecular backscatter coefficient at λ_0 at altitude z,

z_0:   reference height.

5   The reference height z_0 is usually chosen in a way that $\beta_{\lambda_0}^{aer}(z_0) \ll \beta_{\lambda_0}^{mol}(z_0)$. At 355 nm and 532 nm, this condition can be met by seeking the local minimum of the ratio $\beta_{\lambda_0}^{aer}(z_0)/\beta_{\lambda_0}^{mol}(z_0)$ which is usually found in the upper troposphere around 6 to 8 km, and then setting $\beta_{\lambda_0}^{aer}(z_0)$ to zero. At 1064 nm, however, this condition is rather hard to find. Possible ways to calibrate the 1064 nm signal include comparison with

10   column optical thickness measured by sun photometer or using a cirrus cloud with neutral scattering properties as a reference point. Since our site does not operate a sun photometer, we chose the following procedure: For the day where cirrus clouds were present, we chose the same reference height z_0 as for β_{532}^{aer} and β_{355}^{aer}, and adjusted $\beta_{1064}^{aer}(z_0)$ in a way that the neutral scattering properties of the cirrus clouds were

15   reproduced. It turned out that, even though the reference height varied between 4 and 8 km, the "background" backscatter ratio

$$\frac{\beta_{1064}^{aer}(z_0) + \beta_{1064}^{mol}(z_0)}{\beta_{1064}^{mol}(z_0)}$$

converged towards a value of $2.1(\pm 0.7)$. This backscatter ratio was used as the reference value for all measurements at 1064 nm.

Title Page

Abstract | Introduction

Conclusions | References

Tables | Figures

◄◄ | ►►

◄ | ►

Back | Close

Full Screen / Esc

Print Version

Interactive Discussion

In contrast to the extinction coefficient, the determination of the backscatter coefficients is based on the ratio of the Raman and the Rayleigh/Mie return signal. Thus, it can be applied also at altitudes where the laser beam and the telescope field-of-view do not fully overlap, i.e. below 1 km. The extinction coefficient, needed for the extinction correction in Eq. (4), is extrapolated from the measurement at 607 nm to 355 and 1064 nm with the chosen k value. At altitudes below 1 km, where the extinction cannot be measured, it is assumed to be constant.

2.3. Error discussion

The error of the extinction coefficient is mainly determined by the statistical error of the Raman return signal. This error is assumed to be the square root of the absolute count rate and is calculated via the law of error propagation to the error in the extinction coefficient. As Ansmann et al. (1992) pointed out, a rapid change in the aerosol extinction coefficient during the averaged period induces a significant error in the mean extinction coefficient. To avoid such errors, only periods with approximately constant aerosol backscatter signals have been averaged. The error of the backscatter coefficient is mainly determined by the two factors:

(1) The chosen reference height and the chosen aerosol backscatter coefficient at this altitude (we chose zero for 355 and 532 nm). The error of the calibration procedure for 1064 nm, as described above, is determined by the standard deviation of the mean backscatter ratio (2.1 ± 0.7) and was included in the calculation via the law of error propagation.

(2) The calculation of the backscatter coefficient needs the extinction coefficient as an input (see Eq. 4). Since no Raman signals are available for 355 and 1064 nm, the extinction coefficient measured at 532 is extrapolated with the chosen k value, which introduces an additional uncertainty. To assess this uncertainty, backscatter profiles at 355 and 1064 nm were calculated using different k values for the necessary interpolation. Figure 2 gives an example for a calculation of the backscat-

Title Page

Abstract | Introduction

Conclusions | References

Tables | Figures

◄ | ►

◄ | ►

Back | Close

Full Screen / Esc

Print Version

Interactive Discussion

ter coefficient from simulated data (with $k = -1$) at 355 nm, using k values of 0 and -2. Deviations from the initial profile can be more than 100%. At 1064 nm, this effect is much smaller.

Generally, the resulting errors from both error sources exceed the statistical uncertainty by far. As mentioned above, the extinction coefficient is assumed to be constant below the lowest measured value (around 1 km), which causes an additional error, especially if the boundary layer height is very low. Although adjustable neutral density filters are placed in front of the photomultiplier tubes, it could not always been avoided that the photomultiplier used in the 1064 nm channel is overloaded by the strong backscatter signal from the boundary layer. This results in a too low signal above the altitude where the overload occurs.

3. Results

Regular measurements at a fixed time schedule are performed since 1 December 1997. For the usage of the Raman technique, the schedule includes one measurement each Monday after sunset (after 1 January 2000, also Thursday after sunset) with a time window of up 4 hours after sunset. Figure 3 shows the annual distribution of Raman lidar measurements at IAP for the time period between 1 December 1997 and 30 November 2000. In total, of 205 possible measurement days, on 102 days measurements have been performed. This corresponds to a percentage of 49.8%. On the other days, is was either raining or the possibility for rain was too high. On 49 days (23.9%), no clouds were present below 5 km. These days are attributed as "clear" days and will be used for the further aerosol analysis, in order to separate cloud top height and planetary boundary layer height, and to assure that only aerosol properties are discussed.

3.1. Backscatter coefficients and boundary layer heights

Figure 4 shows the annual cycle of the aerosol backscatter coefficient at 532 nm for all measurement days. Shown are monthly mean values. Figure 5 gives the annual cycle for the "clear" days (no clouds below 5 km). The time period displayed in both Figs. 4 and 5 is 1 December 1997 until 30 November 2000. The figures reveal an annual variability of the planetary boundary layer (PBL) height between 1000 and 3000 m, with a minimum in winter and a maximum in summer. The actual time when the maximum is reached varies from year to year: In 1999, the maximum is reached later than during the other 2 years. For the following analysis, the PBL height was defined as that altitude where the aerosol backscatter coefficient (532 nm) decreased to 50% of the mean value below, as shown in Fig. 6. Figure 7 shows the annual cycle of the PBL height for the "clear" days (corresponding to Fig. 5), as monthly averages over the three years. A least-squares fit of the function

$$y = y_0 + a \sin\left(\frac{2\pi}{b}x + c\right),$$

with the constraint that the oscillation period b is 12 months, is also shown, indicating that the average maximum of the PBL height is around mid of July, while the minimum is in mid of January. This means a phase shift of about 25 days with respect to the summer/winter solstices. Here, it has to be reminded that these measurements were taken after sunset. These data can not be assumed to be representative for the maximum PBL height during day-time. In general, the PBL height reaches its maximum around 14:00 local solar time and decreases later through the day. Figure 8 gives the vertical profiles of the backscatter coefficient at 532 nm, where summer (April through September) and winter (October through March) were averaged separately. Although in summer the boundary layer is higher, the highest values of the backscatter coefficients are reached during the winter months. The maximum of the backscatter coefficient during summer is higher than in winter, which reflects the stronger convection during summer. The mean values, in and above the PBL, with their standard deviations

are summarized in Table 2 and plotted vs. wavelength in Fig. 9. Inside the error limit, there is no marked difference in the mean wavelengths dependency between summer and winter, but it appears that the decrease of the backscatter coefficients with wavelength between 355 and 532 nm above the PBL is much steeper that inside the PBL. Since different aerosol types from different origins may contribute to this observation, the question of wavelength dependency and aerosol type will be discussed in detail in Sect. 3.3, where the results of a backtrajectory analysis are presented.

3.2. Extinction coefficients, aerosol optical depths, and lidar ratios

Figure 10 shows the vertical profiles of the extinction coefficient at 532 nm, averaged separately for summer and winter, with bars denoting the standard deviation. The measurements do not cover the whole boundary layer, since the lower measurement height of the lidar system is 1000 m. The scattering of the extinction coefficients is very large, with the mean values scattering around zero above an altitude of 2.5 km. Differences between summer and winter are not recognizable within the error limits. Mean values of the extinction coefficients as well as of the aerosol optical depth (AOD) are given in Table 2. These values describe the region between the upper edge of the boundary layer and the 5-km altitude level. The AOD values of $(0.26 \pm 1.0) \times 10^{-2}$ for summer and $(1.5 \pm 0.95) \times 10^{-2}$ for winter are comparable to the value of 0.012, which is obtained from the Global Aerosol Data Set (GADS) (cf. Hess et al., 1998), and imply that the contribution of the middle free troposphere (well below the tropopause but above the boundary layer) on cloudless days can almost be neglected when discussing total AOD. AOD values over Central Europe at 555 nm, obtained from satellite data, range between 0.1 and 0.6 (Robles Gonzales et al., 2000). AOD values obtained for the planetary boundary layer at the Atlantic coast of the U. S. at 450 nm are in the same order of magnitude (Hartley et al., 2000). Due to the large variations especially in the extinction coefficient, the standard deviation of the mean lidar ratio above the PBL (Table 2) is more than 100% of the mean value for summer and 70% for winter, respectively. In summer, an upper limit of 33 sr can be given, which would

Title Page

Abstract | Introduction

Conclusions | References

Tables | Figures

◄ | ►|

◄ | ►

Back | Close

Full Screen / Esc

Print Version

Interactive Discussion

be in agreement with maritime aerosol (Ackermann, 1998). The mean value for winter of 68 sr is a very reasonable value for continental aerosol (Ackermann, 1998) and also for the "free tropospheric" aerosol component in the Global Aerosol Data Set (Hess et al., 1998). However, the large variability of our data do not allow to draw further
5 conclusions.

3.3. Trajectory analysis

The lidar station Kühlungsborn is located at the southern shore of the Baltic Sea, west (30 km) of the city of Rostock, and east (150 km) of the city of Hamburg. Thus, we would expect the aerosol properties to be dependent on the wind direction. To obtain
10 information about the origin of the air masses, the three-dimensional backward trajectories provided by the German Weather Service (DWD) were analysed by means of cluster analysis. For 46 out of the 49 "clear" measurement days, trajectories were available. The analysis was performed for trajectory arrival heights above Kühlungsborn of 975 hPa (corresponding to 300 m, certainly in the PBL) and 700 hPa (corresponding to
15 3000 m, always above the PBL). The last three days prior to the arrival of the air mass above Kühlungsborn were considered. Following the scheme described in (Romesburg, 1990), the analysis was started with the same number of clusters as trajectories, and continued by decreasing the number of clusters by grouping the two most similar trajectories (those with the lowest square distance) into one cluster. This procedure
20 was repeated up to that point where the sum of the square distances inside the clusters markedly increased. The resulting number of clusters are given in Table 3. At the 700 hPa level, the two dominating clusters contain more then 95% of all measurement days, the other two clusters contain only one trajectory each and were not used in the following analysis. At 975 hPa, four clusters were found which contained at least five
25 trajectories. Figure 11 shows the dominating trajectory directions for both altitudes. At 700 hPa, the dominating wind direction is west. This cluster contains 69.6% of all trajectories, while the second cluster, coming from the south–west, contains 26.2%. At 975 hPa, the western trajectories group into two clusters, characterized by high and

Title Page	
Abstract	Introduction
Conclusions	References
Tables	Figures
◄◄	►►
◄	►
Back	Close
Full Screen / Esc	
Print Version	
Interactive Discussion	

low travelling speed. Additionally, one east-originating cluster and one "anti-cyclonic" cluster is present. In order to find out if a difference in the aerosol properties dependent on the origin of the air masses exists, the backscatter coefficients measured on the days contained in the individual clusters were averaged for both arrival heights. Figure 12 shows the averaged values of the backscatter coefficient at 532 nm along with their standard deviations: Clusters 1, 2, and 3 inside the PBL display almost the same aerosol load, although their origin is completely different. In contrast, cluster 4 (the one with high wind speed from the west) has a markedly higher aerosol load. This may be due to the higher production efficiency of dust and sea salt aerosol at higher wind speeds. For the two clusters analysed at 700 hPa, the total aerosol load does not show a difference between the two clusters within the standard deviation. The right scale in Fig. 12 is expanded by factor of 10 compared to the left, illustrating that the aerosol load (at 532 nm) is by a factor of 10 lower above than inside the PBL.

3.4. Comparison with the Global Aerosol Data Set

Different aerosol types can be distinguished by the spectral dependence of the backscatter coefficients. In order to analyse the wavelength dependence, the averaged data from the individual clusters have been normalized to the value at 532 nm. The result is given in Fig. 13. For clarity, the wavelengths are shifted by 10 nm, centred around the real value. At 975 as well as 700 hPa, the clusters do not show a significant difference in the spectral dependence, but both show a high variability, especially at 355 nm. The mean value at 355 nm of cluster 4 at 975 hPa is lower than the other three, which might fit to the assumption that the higher total aerosol load of cluster 4 is due the higher content of aerosol particles generated by high wind speed (sea salt and dust) which consist of larger particles which have more neutral spectral properties. The steep gradient between 355 and 532 nm measured above the boundary layer may suggest an underestimation of the values at 532 nm, but the variability and measurement uncertainty at 355 nm are so high that the standard deviation is more than 100% of the mean value. Also shown in Fig. 13 are calculated backscatter coefficients for different aerosol types

J. Schneider and R. Eixmann

taken from the software package OPAC (Optical Properties of Aerosols and Clouds), which based on the Global Aerosol Data Set (GADS). Both are freely available on the World Wide Web (Hess et al., 1998). In this data set, the large variability of natural aerosols is reduced by the use of a dataset of typical aerosol components. The size
5 of the individual particles in the OPAC software package is controlled by the relative humidity. We selected from this dataset those aerosol types and components which are likely to be observed at our station, for example "continental", "maritime", "free tropospheric", at their minimum and maximum relative humidities, and compared their calculated backscatter coefficients with our measurements. These backscatter coeffi-
10 cients were also normalized to the measured value at 532 nm. In general, the GADS data agree very well with our data, but mostly the high variability of the measurements does not allow to distinguish between the different aerosol components. The mean values of cluster 4 (in PBL) fit exactly to the aerosol type "maritime clean" in the dry state, while clusters 1, 2, and 3 are in better agreement with the continental aerosol type.
15 For example, the "maritime clean" type at 100% relative humidity can not be brought in agreement with the values from cluster 2, which represents the eastern trajectories. This finding appears plausible. At 700 hPa, no conclusions can be drawn due to the high variability at 355 nm. Summarizing, we observe a slight difference between the clusters in the PBL, but the variability inside the individual clusters is still too large to
20 distinguish between typical aerosol components. It will be necessary to extend the number of clusters in order to reduce the variability, and to extend the data base in order to still have a representative number of trajectories in each cluster.

4. Summary and conclusions

We have presented three complete annual cycles of vertical aerosol profiles between
25 0 and 5 km, and thereby also the annual cycle of the planetary boundary layer height. Mean values for the aerosol backscatter coefficients in and above the PBL are given for 355, 532, and 1064 nm. The backscatter coefficients above the PBL are significantly

lower (by about a factor of 10) than the values inside the PBL. Since the planetary boundary layer has also a diurnal cycle, and our data represent night-time data (taken between sunset and midnight) they will not represent the maximum boundary layer height at our lidar site. The annual cycle, however, is reproduced very well by these after-sunset measurements. The extinction coefficient could only be determined above the PBL for at 532 nm. The inferred optical depth agrees with the value expected from the Global Aerosol Data Set. A trajectory cluster analysis performed on three-day backward trajectories did reveal a difference in the aerosol load in the planetary boundary layer with respect to the wind speed. The air masses arriving with high wind speed from the west contained a markedly higher aerosol load than the other air masses, whose aerosol load was independent from their origin. The comparison with the Global Aerosol Data Set (GADS) showed that our measured aerosol backscatter coefficients do agree with most of the expected aerosol types. The variability inside the clusters, especially at 355 nm, allows only a few conclusions: For example, the "maritime clean" aerosol type at 100% relative humidity can be excluded for the air masses originating from the east, which is a plausible finding. In contrast, the air masses of westerly origin traveling at high wind speed agree very well with the aerosol type "maritime clean". Future measurements and analyses will have to include the extinction coefficient at least at a second wavelength, in as well as above the PBL, and also the daytime data to record the PBL development fully. If these measurements can not be realized by the use of the inelastic Raman scattering, better input data for the lidar ratio are required.

References

Ackermann, J.: The extinction-to-backscatter ratio of tropospheric aerosol: A numerical study, J. Atmos. Oceanic Technol., 15, 1043–1050, 1998.

Alpers M., Eixmann, R., Höffner, J., Köpnick, T., Schneider, J., and von Zahn, U.: The Rayleigh/Mie/Raman Lidar at IAP Kühlungsborn, J. Aerosol Sci., 30, Suppl. 1, 637–638, 1999.

Ansmann, A., Riebesell, M., and Weitkamp, C.: Measurement of atmospheric aerosol extinction profiles with a Raman lidar, Opt. Lett. 15, 746–748, 1990.

Ansmann, A., Wandinger, U., Riebesell, M., Weitkamp, C., and Michaelis, W.: Independent measurement of extinction and backscatter profiles in cirrus-clouds by using a combined Raman elastic-backscatter lidar, Appl. Opt., 31, 7113–7131, 1992.

Bösenberg, J., Alpers, M., Böckmann, C., Jäger, H., Matthias, V., Trickl, T., Wandinger, U., und Wiegner, M.: A Lidar Network for the Establishment of an Aerosol Climatology, in: Proceedings of 19. ILRC, Annapolis, 1998, (Eds) Singh, U. and Ismail, S., NASA/CP-1998-207671/PT1, 23–24, 1998.

Bösenberg, J., Ansmann, A., Baldasano, J. M., Balis, D., Böckmann, Ch., Calpini, B., Chaikovsky, A., Flamant, P., Hagard, A., Mitev, V., Papayannis, A., Pelon, J., Resendes, D., Schneider, J., Spinelli, N., Trickl, Th., Vaughan, G., Visconti, G., and Wiegner, M.: EARLINET: A European Aerosol Research Lidar Network, in: Advances in Laser Remote Sensing, (Eds) Dabas, A., Loth, C., and Pelon, J., ISBN 2-7302-0798-8, 155–158, 2001.

Fernald, F. G.: Analysis of atmospheric lidar observations: some comments, Appl. Opt. 23, 652–653, 1984.

Ferrare, R. A., Melfi, S. H., Whiteman, D. N., Evans, K. D., and Leifer, R.: Raman lidar measurements of aerosol extinction and backscattering 1. Methods and comparisons, J. Geophys. Res., 103, 19 663–19 672, 1998.

Hartley, W. S., Hobbs, P. V., Ross, J. L., Russell, P. B., and Livingston, J. M.: Properties of aerosols aloft relevant to direct radiative forcing off the mid-Atlantic coast of the United States, J. Geophys. Res., 105, 9859–9885, 2000.

Hess, M., Koepke, P., and Schult, I.: Optical properties of aerosols and clouds: The software package OPAC, Bull. Amer. Meteor. Soc., 79, 831–844, 1998.

Klett, J. D.: Stable analytic inversion solution for processing lidar returns, Appl. Opt., 20, 211–220, 1981.

Raman lidar measurements of tropospheric aerosols

J. Schneider and R. Eixmann

Title Page

Abstract | Introduction

Conclusions | References

Tables | Figures

◄◄ | ►►

◄ | ►

Back | Close

Full Screen / Esc

Print Version

Interactive Discussion

Klett, J. D.: Lidar inversion with variable backscatter/extinction ratios, Appl. Opt., 24, 1638–1643, 1985.

Robles Gonzales, C., Veefkind, J. P., and de Leeuw, G.: Aerosol optical depth over Europe in August 1997 derived from ATSR-2 data, Geophys. Res. Lett., 27, 955–958, 2000.

5 Romesburg, H. Ch.: Cluster analysis for researchers, R. E. Krieger Publishing, Malabar, Florida, pp. 335, 1990.

Sasano, Y., Browell, E. V., and Ismail, S.: Error caused by using a constant extinction/backscattering ratio in the lidar solution, Appl. Opt., 24, 3929–3932, 1985.

Title Page

Abstract | Introduction

Conclusions | References

Tables | Figures

◄ | ►

◄ | ►

Back | Close

Full Screen / Esc

Print Version

Interactive Discussion

Table 1. Technical data of the IAP RMR Lidar

Transmitter		Receiver	
Laser type	seeded Nd:YAG	Telescope type	parabolic
Wavelengths	355, 532, 1064 nm	Focal lengths	120 cm
Pulse energies	200, 400, 500 mJ	Active diameter	50 cm
Repetition rates	30 pps	Fibre diameter	1 mm
Pulse lengths	10, 13, 18 nsec	Num. Aperture	0.22
		Field-of-view	0.83 mrad

Detection channels

Channel No.	1	2	3	4
Interference filters				
Central wavelength	354.61	532.09	607.44	1064.14
Full width at half max.	0.92	0.32	0.36	1.02
Transmission	44%	64%	69%	76%
Manufacturer	BARR	BARR	BARR	BARR
Photomultipliers				
Manufacturer	Hamamatsu	Hamamatsu	Hamamatsu	Hamamatsu
Type	4220P (selected)	4632P (selected)	4632P (selected)	R3236 (selected), cooled
Data acquisition mode	100 MHz photon counting	100 MHz photon counting	100 MHz photon counting	100 MHz photon counting

Raman lidar measurements of tropospheric aerosols

J. Schneider and
R. Eixmann

**Table 2.** Mean values of backscatter and extinction coefficients, optical depths and lidar ratios in and above the PBL

	$\overline{\beta}_{355\,nm}$(m^{-1}sr^{-1})	$\overline{\beta}_{532\,nm}$(m^{-1}sr^{-1})	$\overline{\beta}_{1064\,nm}$(m^{-1}sr^{-1})	$\overline{\alpha}_{532\,nm}$(m^{-1})	$\overline{AOD}_{532\,nm}$	$\overline{LR}_{532\,nm}$(sr)
In PBL						
Summer	$(3.2\pm1.3)\times10^{-6}$	$(1.2\pm0.49)\times10^{-6}$	$(4.9\pm0.98)\times10^{-7}$	–	–	–
Winter	$(2.0\pm1.4)\times10^{-6}$	$(1.7\pm0.89)\times10^{-6}$	$(6.7\pm1.4)\times10^{-7}$	–	–	–
Above PBL						
Summer	$(5.2\pm2.5)\times10^{-7}$	$(1.8\pm0.59)\times10^{-7}$	$(7.3\pm1.2)\times10^{-8}$	$(0.48\pm2.8)\times10^{-6}$	$(0.26\pm1.0)\times10^{-2}$	4.8 ± 28
Winter	$(3.1\pm1.6)\times10^{-7}$	$(7.2\pm2.7)\times10^{-8}$	$(6.5\pm2.0)\times10^{-8}$	$(4.9\pm2.4)\times10^{-6}$	$(1.5\pm0.95)\times10^{-2}$	68 ± 42

Title Page

Abstract   Introduction

Conclusions   References

Tables   Figures

◄◄   ►►

◄   ►

Back   Close

Full Screen / Esc

Print Version

Interactive Discussion

J. Schneider and
R. Eixmann

Table 3. Results of the trajectory cluster analysis. Clusters containing only one trajectory were not included in the data analyis

Level	Cluster	# of Trajectories in cluster	Percentage
975 hPa	1	25	56.8
	2	9	20.0
	3	5	11.1
	4	6	13.3
700 hPa	1	32	69.6
	2	12	26.1
	3	1	2.2
	4	1	2.2
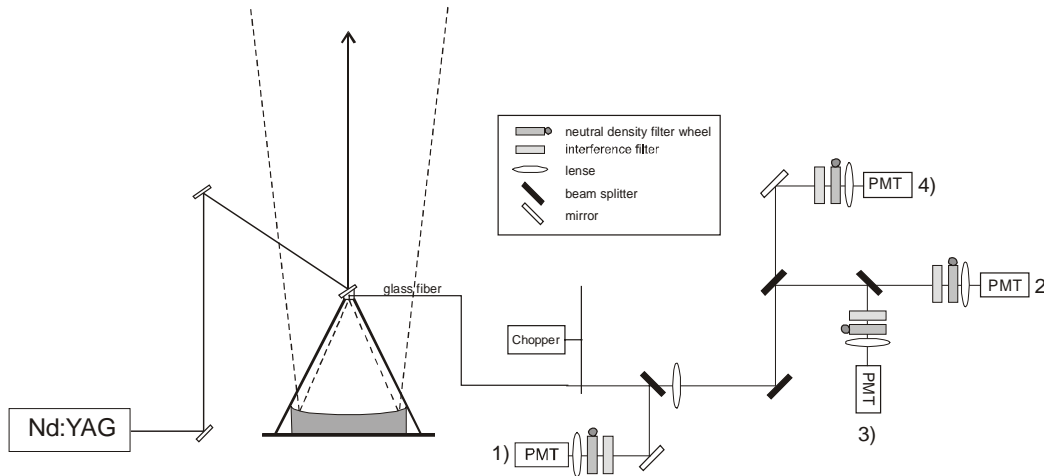
Fig. 1. Setup of the IAP RMR lidar. Only the detection channels used in this work are shown. Technical details are given in Table 1.
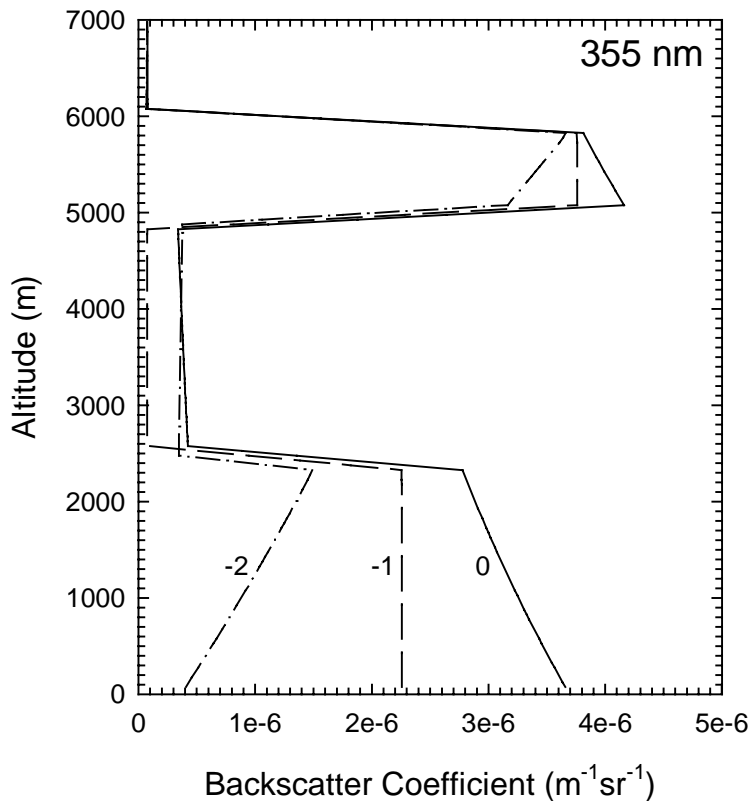
Fig. 2. Backscatter coefficient at 355 nm, calculated from synthetic data using Eq. (4), with k values of -2, -1, and 0. The curve labeled "-1" represents the input data. The difference in the boundary layer can be more than 100%.
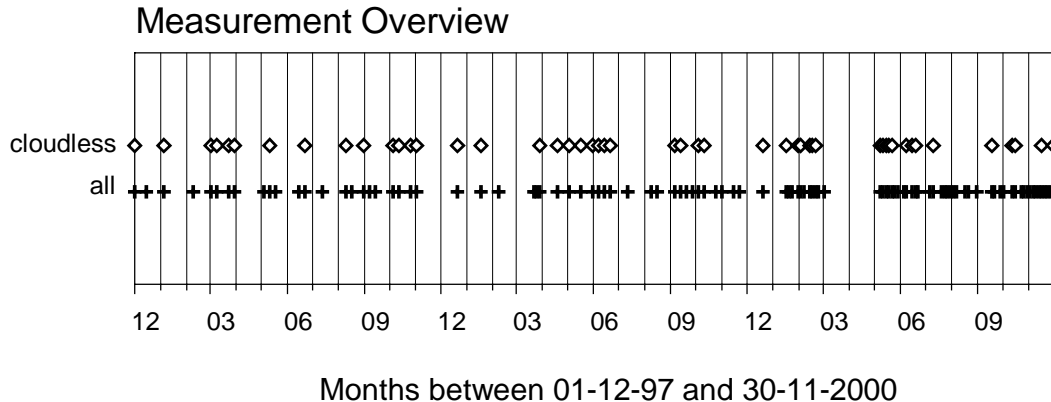
Fig. 3. Overview of the measurements performed on the climatological basis within the German Lidar Network and the European Aerosol Lidar Research Network. "All" denotes all climatological measurements taken between 1 December 1997, and 30 November 2000, "cloudless" denotes all measurements without clouds below 5 km.
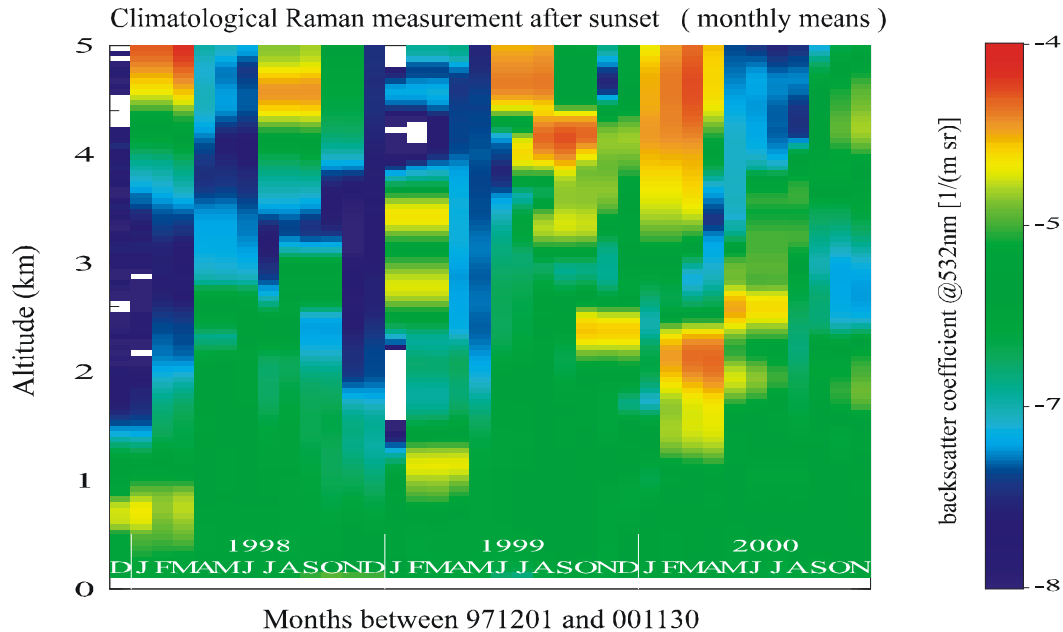
Fig. 4. Annual cycle of aerosol backscatter coefficients at 532 nm for all measurement days. Shown are monthly values, smoothed with a running mean over three months.
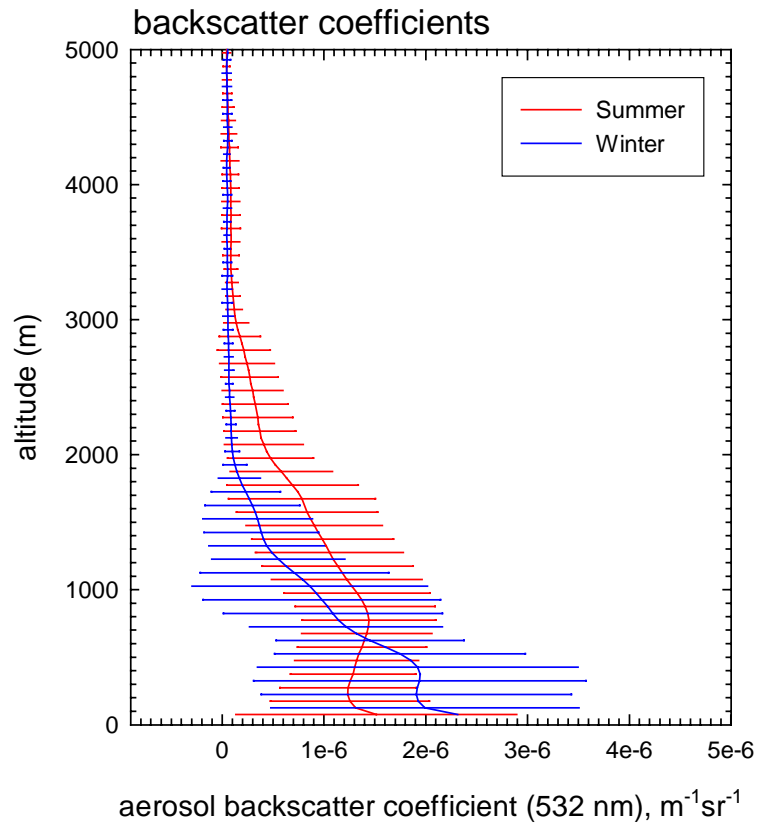
Raman lidar measurements of tropospheric aerosols

J. Schneider and R. Eixmann
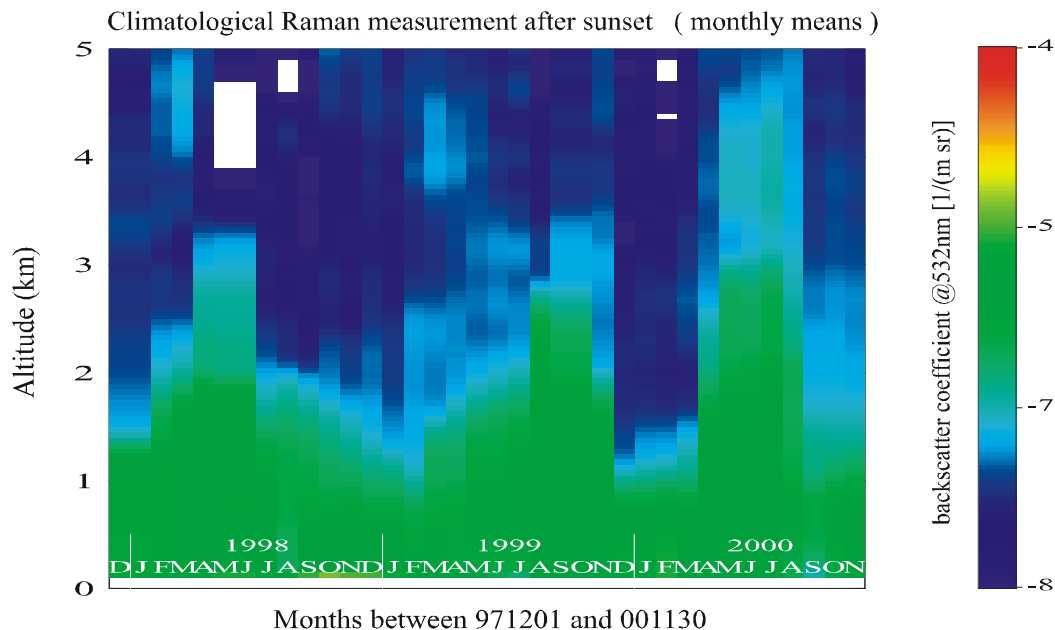
Fig. 5. Annual cycle of aerosol backscatter coefficients (532 nm), cloudless day only. Shown are monthly mean values, smoothed with a running mean over three months. White areas indicate values below the detection limit.

J. Schneider and
R. Eixmann
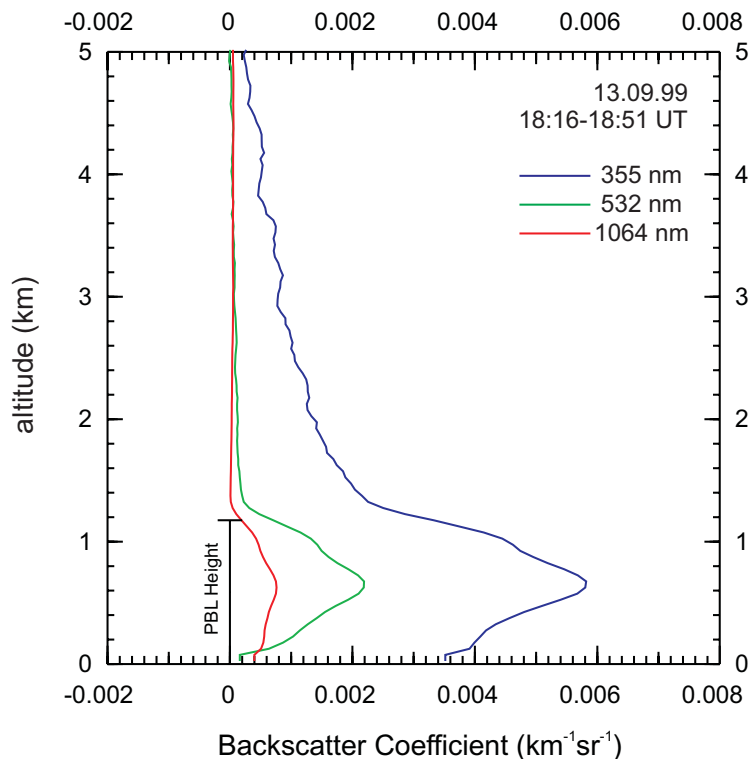
Fig. 6. Illustration of the definition of the PBL height used in this work: The upper end of the PBL is defined as that altitude z where the mean backscatter coefficient decreases to half of the mean value between the lowest measurement level and z. To determine the PBL height, the data measured at 532 nm have been used.

Title Page

Abstract Introduction

Conclusions References

Tables Figures

◀◀ ▶▶

◀ ▶

Back Close

Full Screen / Esc

Print Version

Interactive Discussion
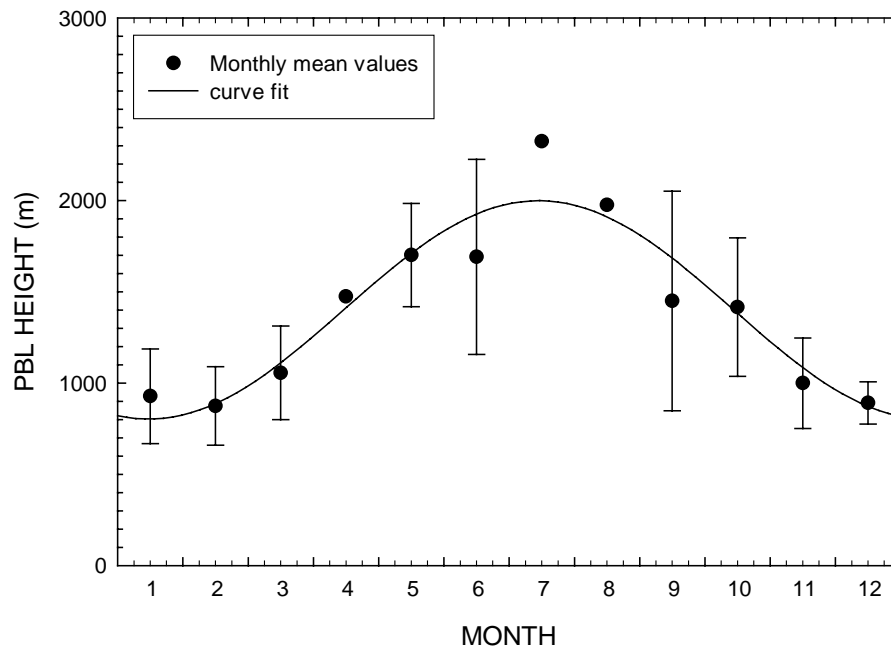
Fig. 7. Annual cycle of the monthly mean planetary boundary layer height, inferred from the backscatter coefficient at 532 nm. The data points represent monthly mean values averaged over the 3 years. The bars represent standard deviations. Points with no bars represent the only measurement in this month. Also shown is a least-squares fit of the function $y = y_0 + \sin\left((2p/b)x + c\right)$, with the constraint that $b = 12$ months.

backscatter coefficients

Fig. 8. Vertical profiles of the backscatter coefficient at 532 nm, separately averaged for summer (April through September) and winter (October through March).

J. Schneider and
R. Eixmann

backscatter coefficients

Fig. 9. Spectral dependence of mean backscatter coefficients inside and above the PBL, averaged separately for summer (April through September) and winter (October through March).
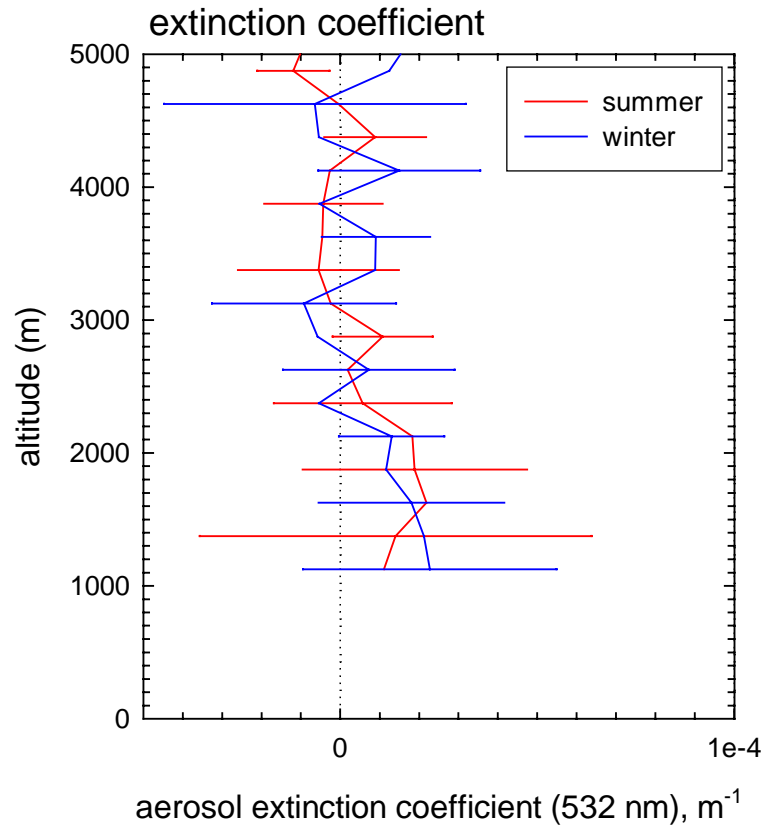
Fig. 10. Vertical profiles of the extinction coefficient at 532 nm, separately averaged for summer (April through September) and winter (October through March).

Fig. 11. Map of central Europe, showing the results of the cluster analysis of the backward trajectories arriving above Kühlungsborn (54° N, 12° E) at 19:00 UT on the measurement days. Two arrival heights are shown. Gray lines: 700 hPa (above PBL), black lines: 975 hPa (inside PBL).
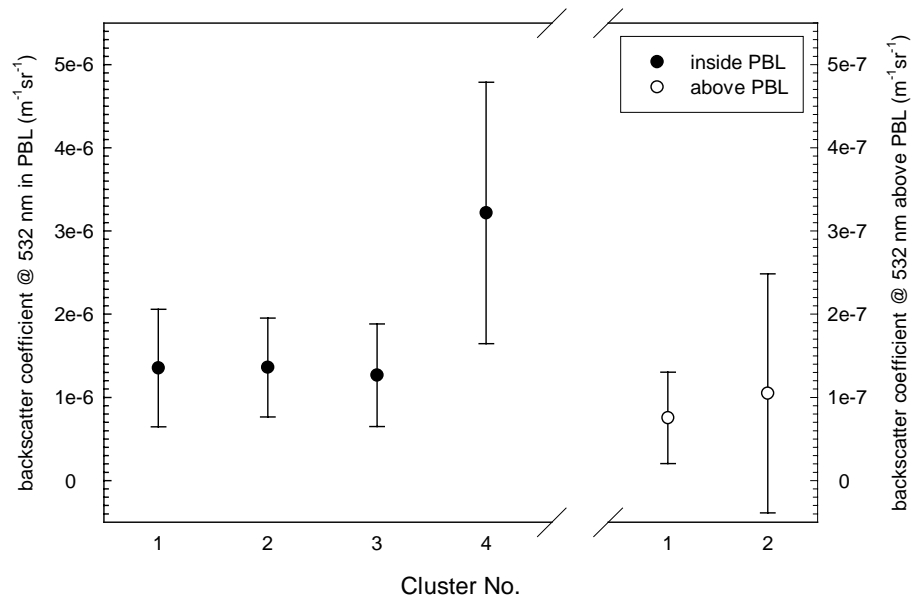
Fig. 12. Mean aerosol backscatter coefficients at 532 nm measured in the individual clusters given in Fig. 11. The right scale is expanded by a factor of 10 compared to the left. Cluster 4 (975 hPa) shows a markedly higher aerosol load than the other 3 clusters at 975 hPa. At 700 hPa, no significant difference can be found.

Title Page

Abstract · Introduction

Conclusions · References

Tables · Figures

◄ · ►

◄ · ►

Back · Close

Full Screen / Esc

Print Version

Interactive Discussion
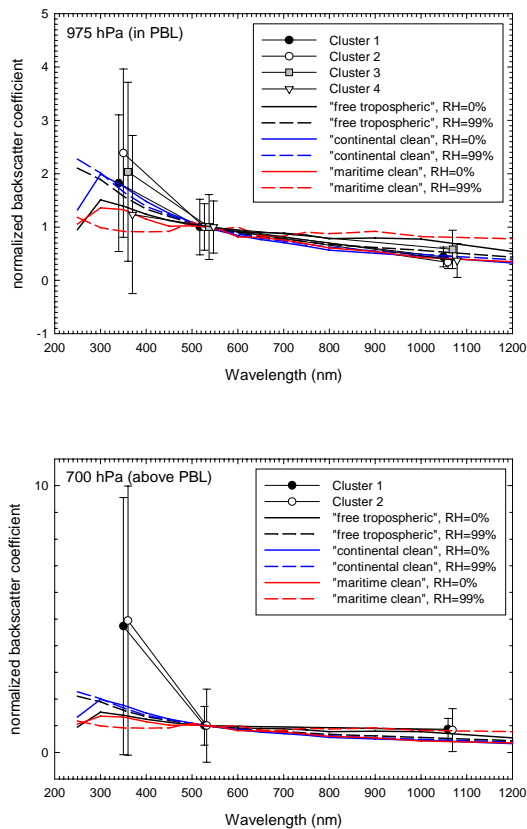
Fig. 13. Mean backscatter coefficients measured in the individual clusters given in Fig. 11, normalized to the value measured at 532 nm. Upper panel: in PBL, lower panel: above PBL. The error bars indicate the standard deviation inside the clusters. For clarity, an offset of 10 nm was added to wavelengths, centered around the real value. Also shown are selected aerosol types from the Global Aerosol Data Set (GADS).